



Research Article

A Robust Sequential Quadratic Programming Optimization Technique for Proportional-Integral-Derivative Controller of Boost Converter in Brushless Direct Current Motor Considering Renewable Energy Sources

Eki Roviando ^{1,*}, Bhre Wangsa Lenggana ², Khairunnisa ³, Luki Septya Mahendra ⁴, Ari Prasetyo ¹, Catur Harsito ^{1,5}

¹Department of Mechanical Engineering, Vocational School, Universitas Sebelas Maret, Surakarta, 57126 Indonesia

²Department of Mechanical Engineering, Universitas Jenderal Soedirman, Purwokerto, 53122, Indonesia

³Department of Electrical and Electronic Engineering, Vocational Faculty, Universitas Negeri Yogyakarta, Yogyakarta, 55281, Indonesia

⁴Department of Electrical Engineering, Politeknik Elektronika Negeri Surabaya, Surabaya, 60111, Indonesia

⁵Mechanical, Computer, Industrial Management Engineering Department, Kangwon National University, Samcheok, 25913, Republic of Korea

*Corresponding author: ekirovianto@staff.uns.ac.id, Tel.: +62271-664126, Fax.: +62271-664126

Abstract: The development of renewable energy has had a positive impact on reducing the level of fossil fuel emissions. One of the renewable energies that currently has a fairly high level of efficiency is Photovoltaic (PV). Motors supplied by PV have a low starting voltage and cause voltage fluctuations, reducing the stability and performance of the motor. One method that can be used to reduce voltage fluctuations is to control its stability. This can be achieved by adding a boost converter controlled by an optimized Proportional Integral Derivative (PID). Several methods are often used to find the right PID value, including the trial-and-error method and the numerical optimization method. This paper discusses the optimization of PID tuning on boost converters and Brushless Direct Current (BLDC) motors using the Sequential Quadratic Programming (SQP) method. Tuning using SQP provides an overshoot value of 0% and a completion time of 480 s, which is much smaller than the metaheuristic-based ones, such as Geometric Mean Optimizer (GMO) 379 s and Firefly Algorithm (FA) 1108 s. In addition, the simulation time obtained on SQP is 13.25 and 16.41 times faster than GMO and 16.41 times faster than FA. Considering the performance in terms of the integral of time-weighted absolute error (ITAE), SQP has a better performance by 1018555 compared to the metaheuristic method, which has a performance of 1097300. This difference indicates that SQP, which is a metaheuristic method, produces a more optimal ITAE value by 7.18% compared to FA and 9.64% compared to GMO.

Keywords: BLDC motor; Boost converter; PID controller; Renewable energy; Robust SQP optimization

This work was supported by 'Universitas Sebelas Maret' funded by 'Penelitian Unggulan Terapan (PUT) 2024 under contract number 194.2/UN27.22/PT.01.03/2024'

<https://doi.org/10.14716/ijtech.v16i5.7269>

Received August 2024; Revised October 2024; Accepted January 2025

1. Introduction

The global shift toward renewable energy sources has been instrumental in mitigating fossil fuel emissions' environmental impact. Among these renewable energy technologies, PV systems have emerged as a highly efficient solution. Solar photovoltaic (PV) technology harnesses sunlight and converts it directly into electricity through the PV effect, making it a clean and sustainable energy source ([Ajiwiguna and Kirom, 2024](#); [Jamahori et al., 2024](#); [Saaïd et al., 2018](#); [Aiman Setiawan, 2017](#)).

However, the integration of PV systems with motors poses challenges due to their low starting voltage and inherent voltage fluctuations, leading to compromised stability and performance. Various methods have been explored to address these challenges, with one promising approach being the integration of boost converters optimized through proportional-integral-derivative (PID) control ([Malla et al., 2022](#); [Ben Safia et al., 2021](#); [Munisekhar et al., 2020](#); [Mohammed and Farah, 2019](#)). Traditional tuning methods for PID controllers, such as trial and error and numerical optimization, are often time-consuming and inefficient.

The global shift toward renewable energy sources has become an important cornerstone in efforts to reduce the negative impact of fossil fuel emissions on the environment. In this context, renewable energy technologies, especially PV systems, have emerged as a highly efficient and promising solution ([Hasanah et al., 2024](#); [Kumar and Vinaykumar, 2023](#); [Jia et al., 2019](#)). However, the integration of a PV system with a motor is a major challenge, especially due to the presence of low starting voltages and naturally occurring voltage fluctuations, which directly impact the stability and performance of the entire system ([Anshory et al., 2024](#); [Osman et al., 2022](#); [De et al., 2020](#)). Various strategies and methods have been studied to overcome this complexity, and among them, a promising approach is the integration of optimized boost converters via PID control ([Aguila-Leon et al., 2021](#); [Devaraj et al., 2021](#); [Khleaf et al., 2019](#)).

A PID is a type of controller primarily used for error correction. It addresses voltage deviations occurring between the system output and the PID controller input for controlling voltage in a system. PID is relatively simple compared to other control methods, such as fuzzy logic, artificial neural networks (ANN), and similar approaches. To deliver effective results, it only requires three parameters—proportional, integral, and derivative. These parameters can initially be manually set using random values or through trial-and-error. However, traditional methods for tuning PID parameters, such as trial-and-error methods and numerical optimization, are often faced with time and efficiency constraints ([Aseem and Selva Kumar, 2020](#)). An optimization process is necessary to achieve optimal performance, as better optimization algorithms yield better results. Despite its simplicity, PID can effectively correct system errors, offering robust performance that can be evaluated through parameters such as undershoot, overshoot, rise time, and the speed to reach steady state ([Hekimoğlu and Ekinçi, 2020](#)).

Other control methods, such as fuzzy logic, can also achieve good results; however, they often require numerous rules to ensure optimal performance. The development of these rules involves significant manipulation and adjustment. The construction of a fuzzy logic rule-based is a computationally intensive task that requires considerable effort to attain an accurate and efficient set of rules ([Izci et al., 2022](#); [Ghamari et al., 2022](#)). Similarly, another method, ANN, is versatile and applicable to various systems, but it requires extensive data for the training process, which can be time-intensive ([Devaraj et al., 2021](#); [Khleaf et al., 2019](#)). Furthermore, determining the optimal number of hidden layers and neurons requires additional optimization. Given the lengthy training time required for ANN models, this method may not be suitable for applications requiring immediate results. Hence, for applications demanding timely solutions, PID controllers still outperform other control strategies, particularly when their parameters are fine-tuned.

Therefore, this research aims to examine a new approach using a derivative-based optimization technique, Sequential Quadratic Programming (SQP), in optimizing PID parameters in converters integrated with Brushless Direct Current (BLDC) motors, with the hope of overcoming these challenges more effectively and efficiently. Several derivative-based methods, such as quadratic

and linear programming, offer rapid computation times for finding optimal parameters (Wibowo et al., 2023; Delfianti et al., 2022; Sugiantoro et al., 2021). However, these methods are limited to problems in which the objective function is either quadratic or linear.

Parameterization of solar PV systems is crucial for accurately modeling their behavior and integrating them into the boost converter-BLDC motor system. Parameters such as solar irradiance, temperature, panel orientation, and efficiency are meticulously considered in the research to capture the dynamic nature of solar energy generation (Eleftheratos et al., 2024; Bueso et al., 2022; Liu et al., 2022; Osorio et al., 2019). By incorporating these parameters into the modeling framework, we simulated real-world conditions and evaluated the performance of the proposed robust SQP optimization technique for PID controller design. This comprehensive approach enables a thorough analysis of the system's response to varying solar conditions, ultimately facilitating the development of efficient and reliable renewable energy systems for practical applications. Based on previous research (Anshory et al., 2024).

In addition to the technical challenges faced in integrating a PV system with a motor, the economic aspect is also an important consideration. Although PV technology offers an environmentally friendly and efficient solution, many system owners often face high initial investment costs. Therefore, it is essential to develop methods that can improve the efficiency and performance of PV motor systems without sacrificing stability or requiring large additional investments. In this context, the optimization of PID parameters using the SQP method can be a promising solution because it can produce more optimal tuning with lower computational costs, ultimately reducing the total system operational costs (Khodabakhshian et al., 2012).

The boost converter system's role is also worth noting in this context. The boost converter plays a key role in regulating the PV panel's output voltage to ensure the motor's smooth operation. However, voltage fluctuations can affect overall system stability, especially in the case of motors that require a stable starting voltage to start operation (Alshareef et al., 2021; Obaid et al., 2021; Miqui et al., 2019). Therefore, optimizing the amplifier converter simultaneously with PID tuning is important to achieve an optimal balance between system stability and performance (Ghamari et al., 2022; Izci et al., 2022; Mitra and Rout, 2022; Hekimoğlu and Ekinci, 2020). PID control is needed to stabilize the system, improve response, and reduce errors and flexibility to obtain optimal performance.

In evaluating the effectiveness of the SQP method in optimizing PID parameters, comparisons with alternative methods are also necessary. Genetics-based metaheuristics or DEAs may offer different approaches in the search for optimal parameters (Gao, 2023; Joseph et al., 2022; Janprom et al., 2020). Therefore, comparative analysis between SQP methods and genetics, differential evolution, or genetic algorithms can provide deeper insight into each approach's advantages and disadvantages. Evaluation should not only focus on system performance under simulated conditions but practical testing in the field should also be conducted. Practical testing will provide a better understanding of the effectiveness of PID tuning optimized using the SQP method in real operational conditions. The results of these field tests can be a valuable guide for practical applications in industry and society. In discussing research results, identifying the limitations and weaknesses of the proposed approach is important. Acknowledging limitations and weaknesses can open the door to continued research and further development, as well as provide direction for future research to overcome remaining challenges in PV-motor system integration.

The integration of BLDC motors with PV systems has emerged as a promising approach in the field of renewable energy and efficient power conversion. Photovoltaic systems, which generate electricity from solar energy, can be effectively combined with BLDC motors to power a variety of applications, particularly in the context of water pumping and other sustainable energy solutions. One of them is the application of BLDC in air conditioning systems (Nasruddin and Sinambela, 2015). In addition, this system is applied to a water pump system powered by solar energy. This pump is used in the agricultural sector, but it can also be used in urban areas.

This study focuses on the optimization of PID tuning for boost converters and BLDC motors using the SQP method. SQP offers a computationally efficient alternative to traditional optimization techniques, promising significant reductions in simulation time (Grigoraş et al., 2022; Luo et al., 2022; Mao et al., 2019; Mohasseb et al., 2017). This study contributes to the use of the SQP method to optimize the PID parameters in DC-DC converters integrated with a BLDC motor. This approach offers an innovative solution to improve the stability and performance of PV motor systems, with a focus on better computing time efficiency than traditional methods. In addition, the development of methods that can provide more optimal PID tuning with lower computational costs is necessary, thereby overcoming the time and efficiency constraints often faced by traditional methods. In terms of urgency, this research provides a perspective regarding the need to effectively and efficiently overcome the challenges of PV-motor system integration to increase the adoption of renewable energy technologies and reduce dependence on fossil energy sources that are detrimental to the environment. Thus, this research not only makes a significant contribution to the development of renewable energy technology but also has a positive impact on efforts to mitigate global climate change.

2. Methods

In this research, solar PV systems play a pivotal role in providing renewable energy input to the overall system. Based on previous research (Anshory et al., 2024). Therefore, this study uses fundamental Eqs. (1) and (2), which assume a relationship between basic current interactions and factors that determine the performance of a solar cell.

$$I = I_{ph} - I_d - I_p \quad (1)$$

$$I = I_{ph} - I_0 \left\{ e^{\frac{q(V+R_S I)}{AKT}} - 1 \right\} - \frac{V + R_S I}{R_p} \quad (2)$$

In this context, I represents the total photovoltaic output current, I_{ph} denotes the photocurrent, and I_d refers to the diode current, which can be expressed as Eq. (3)

$$I_d = I_0 \left\{ e^{\frac{q(V+R_S I)}{AKT}} - 1 \right\} \quad (3)$$

Here, I_0 indicates the diode reverse saturation current, I_p is the parallel current, R_p represents the parallel resistance, R_S denotes the series resistance, and q is the electron charge ($1.6 \cdot 10^{-19} \text{C}$). The variable V represents the open-circuit output voltage across the photovoltaic cell, while K stands for the Boltzmann constant. In the short-circuit condition, where I_{ph} can be substituted with the short circuit current I_{SC} , R_p is considered infinite, and the third term in the preceding equation is omitted. Equation (4) provides a clear explanation of the analysis and optimization of solar cell performance under different operational conditions.

$$I = I_{SC} - I_0 \left\{ e^{\frac{q(V+R_S I)}{AKT}} - 1 \right\} \quad (4)$$

The PV output depends on several weather and environmental factors, especially the ambient temperature and solar radiation. This expression describes the relationship between the voltage across a photovoltaic cell and its internal elements, considering the most relevant factors of the diode voltage, current, and series resistance (Eq. (5)).

$$V_{PV} = V_d - I_{PV} R_S \quad (5)$$

Table 1 shows the parameters of the 200 Wp solar panel Grape Solar GS-P-200-CSPE used in this study (MathWorks, 2004).

Table 1 Electrical parameters of the 200 W PV panel

Parameters	Value
Maximum power (W)	200.277
Cells per module (Ncell)	60
Open circuit voltage Voc (V)	36.2
Short-circuit current Isc (A)	7.68
Voltage at the maximum power point Vmp (V)	28.9
Current at the maximum power point Imp (A)	6.93
Temperature coefficient of Voc (%/°C)	-0.37
Temperature coefficient of Isc (%/°C)	0.13

2.1. Boost Converter and BLDC Motor

The boost converter system is a key component in the integration of PV systems with BLDC motors. The boost converter is tasked with changing the output voltage produced by the PV panel into a voltage suitable for driving the BLDC motor with optimal efficiency. Generally, an amplifier converter works by increasing a low input voltage to a higher output voltage. In this context, the amplifier converter system will include technical specifications such as input and output voltages, maximum current, conversion efficiency, and integrated safety features. BLDC motors are a type of electric motor that is increasingly popular because of their efficiency, reliability, and good control. BLDC motors do not have friction brushes like conventional DC motors, which makes them more durable and requires less maintenance. A description of a BLDC motor will include its physical and electrical characteristics, such as the number of phases, maximum torque, maximum rotational speed, and control configuration used. In addition, the system description will cover the interaction between the boost converter and the BLDC motor, including how the boost converter's output voltage is controlled and adjusted to match the BLDC motor's operational requirements. This section includes an explanation of how PID control is integrated with the system to ensure voltage stability and optimal motor performance. Thus, this system description will provide a comprehensive understanding of how boost converters and BLDC motors interact in PV-motor integration applications and how PID control is used to optimize the overall system performance.

2.2. SQP Optimization

The SQP method is an optimization technique used to solve nonlinear optimization problems with nonlinear constraints. The basic principle of SQP involves iteration to gradually improve the solution until it converges to the optimal solution. In the initial stage, SQP starts by guessing the starting point and updating the point using iterative steps. Each iteration involves the following steps: first, a quadratic model of the original optimization problem around the point being evaluated is defined; second, the resulting sub-quadratic problem is solved to generate search directions; and third, a search step is performed in the given direction to update the points and continue the iteration. This process is repeated until the convergence criteria are met or an optimal solution is found.

In the context of this research, SQP is applied to solve optimization problems involving tuning PID parameters in amplifier converters and PID control in BLDC motors. Therefore, this section also discusses how the optimization problem is structured to consider the optimization objectives, constraints, and decision variables. Then, SQP is applied to solve this problem by considering the mathematical structure of the problem and using iterative techniques to reach an optimal solution. Thus, the explanation of the basic principles and implementation of SQP in this research will provide a deep understanding of how this optimization method is applied to overcome challenges in PV-motor system integration.

Figure 1 The general flowchart of the SQP method is proposed. The algorithm can be summarized as follows:

$$\begin{aligned} &\min f(x) \\ &\text{Subject to } g_b(x) \leq 0, b = 1, \dots, m \end{aligned}$$

where x represents the PID controller parameters that should be optimized, $f(x)$ represents the objective function given in Eq. (6), and $g(x)$ represents the inequality constraint. The algorithm proposed in this paper is as follows (Khodabakhshian et al., 2012):

At iteration $k = 1$,

Step 1: The Lagrangian of this problem is defined as follows:

$$L(x, \alpha) = f(x) + \sum_{b=1}^m \alpha_b g_b(x) \quad (6)$$

where α is the vector of the approximate Lagrange multipliers. With x_n as the PID controller gains in the current iteration and the current approximate Hessian (H_n). The QP is defined as:

$$\min q(d) = \frac{1}{2} d^T H d + \nabla f(x)^T d \quad (7)$$

where d is the current iteration for the search direction. The matrix H is a positive definite approximation of the Hessian matrix of the Lagrangian function ($H = \nabla_{xx}^2 L$). To attain an optimal point, the parameters must satisfy the Kuhn-Tucker (KT) condition, defined by the Kuhn-Tucker point as $\nabla_x L(x^*, \alpha^*) = 0$. The x^* and α^* are the optimum points.

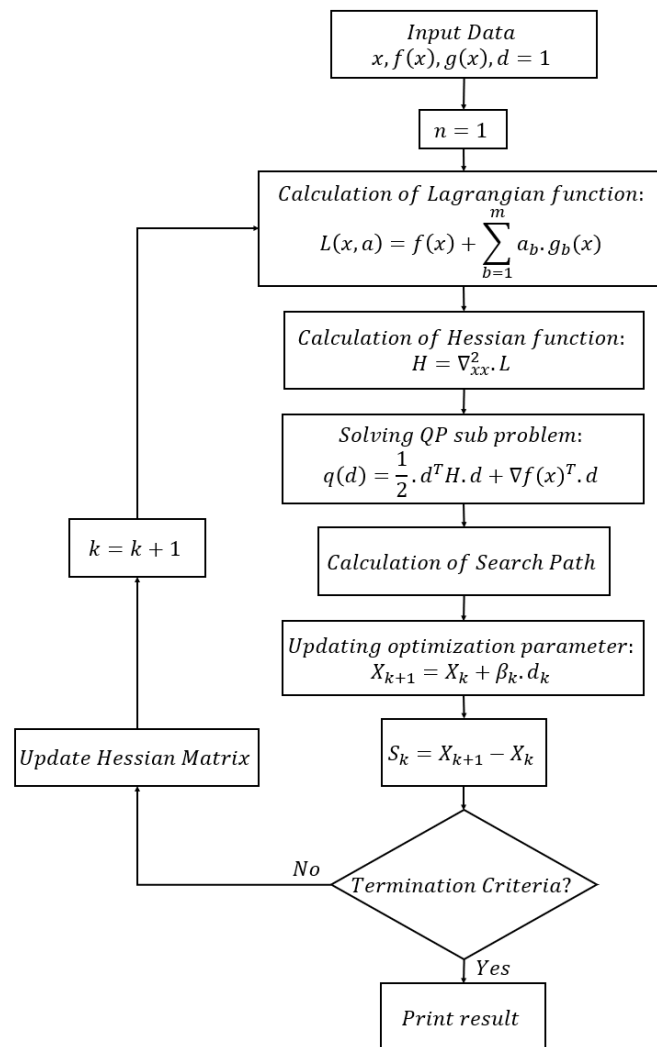


Figure 1 Flowchart of the SQP method

Step 2: The calculation of the next iterative point based on the vector d_k , produced as a result of the solution of the QP sub-problem, is performed. The first is a merit function $\psi(x)$ is defined as follows:

$$\psi(x) = f(x) + \sum_{b=1}^m r_b \cdot g_b(x) \quad (8)$$

where r_b is known as the penalty parameter and is initially set to $\frac{\partial f(x)}{\partial g_b(x)}$.

Then, the next x_{k+1} will be determined as follows:

$$X_{k+1} = X_k + \beta_k \cdot d_k \quad (9)$$

where β_k is the step length parameter and is determined to sufficiently reduce the merit function $\psi(x)$.

Step 3: The Hessian approximation H_{k+1} is updated using the Broyden, Fletcher, Goldfarb, and Shanno (BFGS) (Kang & Youn, 2019) formula:

$$H_{k+1} = H_k + \frac{q_k q_k^T}{q_k^T S_k} - \frac{H_k^T H_k}{S_k^T H_k S_k} \quad (10)$$

where $S_k = X_{k+1} - X_k$ and q_k are given by either of the following equations: Using this formula, the Hessian approximate H remains positive definite.

$$q_k = \nabla_x L(X_{k+1}, \beta_k) - \nabla_x L(X_k, \beta_k) \quad (11)$$

$$q_k = \Delta f(X_{k+1}) + \sum_{b=1}^m \beta_b \cdot \Delta g_b(X_{k+1}) - [\Delta f(X_k) + \sum_{b=1}^m \beta_b \cdot \Delta g_b(X_k)] \quad (12)$$

Step 4: when the s_n becomes a very small value, the program can be stopped. Otherwise, the value of k will be $k = k + 1$, and the algorithm should start again from step 1 and proceed as described above.

2.3. Mathematical modeling of the boost converter and the BLDC motor

Boost converters are essential components in renewable energy systems, particularly in applications such as PV systems and wind turbines. They are used to efficiently increase the voltage levels to match the load or grid requirements. The mathematical model of a boost converter typically includes equations describing the relationship between input and output voltages, currents, and the duty cycle of the switching device (such as a MOSFET or IGBT). These models often consider parameters such as the inductor and capacitor values, switching frequency, and efficiency.

The boost converter's dynamic behavior is crucial for designing effective control strategies, as it directly impacts the system's stability, transient response, and efficiency. Modeling techniques may involve state-space representations, transfer functions, or circuit-based simulations using tools such as SPICE. Figures 2–4 depict the schematic of the boost converter.

The basic operation of a boost converter can be described as follows:

$$V_L = L \frac{di_L}{dt} \quad (13)$$

$$i_C = C \frac{dv_C}{dt} \quad (14)$$

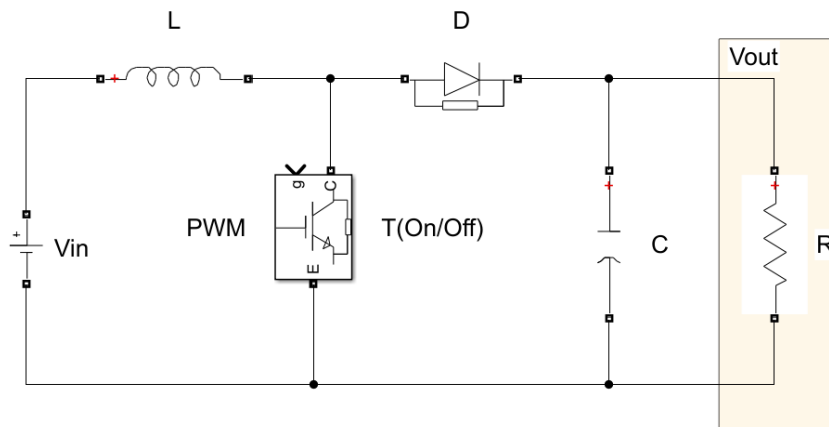


Figure 2 Schematic of the Boost Converter

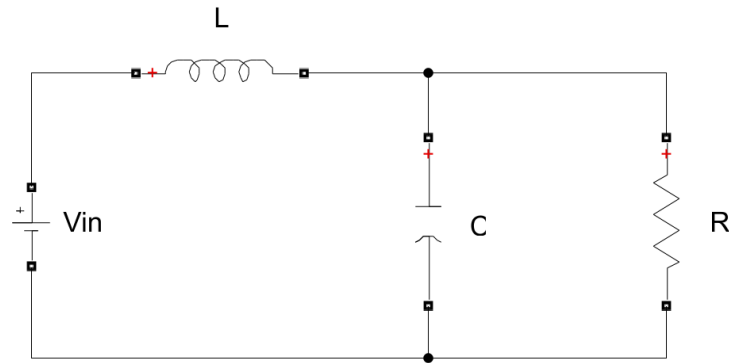


Figure 3 Boost converter t-On condition

The working process of the DC-DC Boost Converter begins with the switching process, which produces two circuits, as shown in Eqs. (13)-(15) below. The Boost Converter equation in the ON position is defined as follows:

$$V_L = V_{in} \times PWM \quad (15)$$

Meanwhile, the position of the DC-DC converter in the OFF is shown:

$$V_L = (V_{in} - V_{out}) \times PWM \quad (16)$$

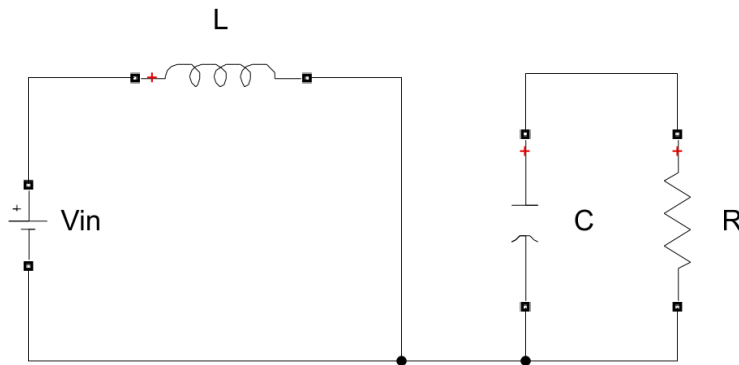


Figure 4 T-Off condition of the boost converter

The switching process between the ON and OFF positions is determined by the *PWM* switching frequency and duty cycle as follows:

$$PWM = \frac{(V_{out} - V_{in})}{V_o} f_{pwm}^{-1} \quad (17)$$

The current flowing through the inductor and capacitor is as follows:

$$i_L = \frac{1}{L} \int V_L dt \quad (18)$$

$$i_C = i_L - i_R \quad (19)$$

The voltage equation on the capacitor is defined as follows:

$$V_C = \frac{1}{C} \int i_C dt \quad (20)$$

The total impedance functions are given by Eqs. (21)-(25). The DC-DC Boost converter is modeled in the S-domain using the transfer function modeling technique as follows:

$$Z_{total} = Z_1(s) + Z_2(s) \quad (21)$$

$$Z_1(s) = \frac{V_{in}(s)}{I(s)} = \left[R \frac{1}{C_s} \right] + L_s \quad (22)$$

$$\frac{V_{in}(s)}{I(s)} = \frac{RCLs^2 + Ls + R}{RCs + 1} \quad (23)$$

$$I(s) = \frac{RCs + 1}{RCLs^2 + Ls + R} V_{in}(s) \quad (24)$$

$$Z_2(s) = \frac{V_{out}}{I(s)} = \frac{R}{RCs + 1} \quad (25)$$

The final equation of the transfer function for the DC-DC Boost converter is given by Eq. (26). The final equation is defined as

$$\frac{V_{out}}{V_{in}} = \frac{R}{RCLs^2 + Ls + R} \quad (26)$$

These equations describe the relationship between the input and output voltages, the output current, the inductor current, and the Pulse Width Modulation (*PWM*) of the boost converter. Here, V_{in} is the input voltage, V_{out} is the output voltage, R_{load} is the load resistance, and L is the boost converter's inductance. Table 2 shows the parameters of the boost converter used in this system (Anshory et al., 2024).

Table 2 DC-DC converter parameters

Parameter	Symbol	Value
Resistance	L	100 Ω
Inductance	R	470.000 <i>mH</i>
Capacitance	C	470 μF

BLDC motors are widely used in various applications because of their high efficiency, reliability, and controllability. In the context of renewable energy systems, BLDC motors are commonly employed in applications such as electric vehicles, wind turbines, and micro-hydro generators. The mathematical model of a BLDC motor typically comprises equations describing the electromagnetic, mechanical, and electrical characteristics. The electromagnetic dynamics of a BLDC motor involve the relationships between the rotor position, electromagnetic torque, and currents flowing through the motor windings. These dynamics are often described using equations derived from electromagnetism and motor construction principles. Additionally, the mechanical dynamics of the BLDC motor include equations governing the rotational motion, such as the relationship between torque, speed, and inertia. These equations account for factors such as friction, load torque, and mechanical losses.

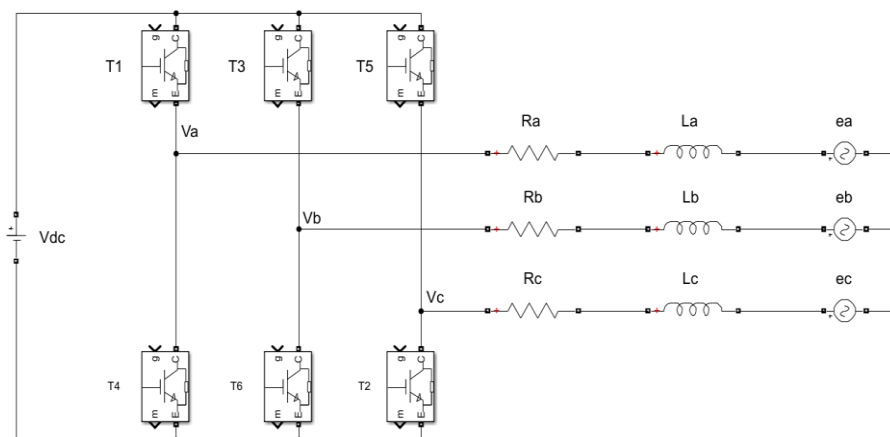


Figure 5 Schematic of the BLDC model

The electrical characteristics of the BLDC motor encompass equations defining the voltage-current relationship, back electromotive force (EMF), and motor winding resistance. These equations are crucial for understanding how the motor responds to control signals and external

loads. The equivalent circuit of the BLDC motor is shown in Figure 5. By accurately modeling both the boost converter and the BLDC motor, researchers can analyze the interactions between these components and design optimal control strategies to achieve desired performance metrics, such as efficiency, transient response, and stability. Moreover, such models serve as valuable tools for simulation-based studies and experimental validation, facilitating the development and deployment of RE systems.

The mathematical model of a BLDC motor typically includes the following equations governing its electromagnetic, mechanical, and electrical dynamics by Eq. (27) – (29):

$$V_a = I_a R_a + L_a \frac{di_a}{dt} + e_a \quad (27)$$

$$V_b = I_b R_b + L_b \frac{di_b}{dt} + e_b \quad (28)$$

$$V_c = I_c R_c + L_c \frac{di_c}{dt} + e_c \quad (29)$$

The mechanical time constant for the mathematical equation is defined as follows:

$$\tau_m = \frac{RJ}{K_e K_t} \quad (30)$$

The electrical time constant is shown:

$$\tau_e = \frac{L}{3R} \quad (31)$$

$$K_E = \frac{3RJ}{K_T \tau_m} \quad (32)$$

For the BLDC motor, the equation is defined as

$$G(s) = \frac{\omega_m}{V_s} = \frac{1/K_e}{\tau_m \tau_e s^2 + \tau_m s + 1} \quad (33)$$

where K_t is the torque constant, I_a, I_b , and I_c are the armature current per phase, e_a, e_b , and e_c are return EMF per phase, K_e is the back EMF constant, ω_m is the rotor angular velocity, V_s is a voltage source, J is the rotor's moment of inertia, $R = R_a = R_b = R_c$ is armature resistance, $L = L_a = L_b = L_c$ is the armature self-inductance, τ_m is mechanical torque, τ_e is the electrical torque. These equations describe the relationship between the electromagnetic torque, back EMF, rotor angular velocity, and mechanical dynamics. They are essential for understanding the motor's behavior under different operating conditions and designing control strategies to achieve the desired performance objectives. The nominal voltage of the BLDC motor is 24 volts with 8 poles. Table 3 shows the BLDC motor parameters (Anshory et al., 2024).

Table 3 BLDC motor parameters

Parameter	Symbol	Value
Torque Constant	K_t	0.0521 Nm/A
Back EMF constant	K_e	0.0521 V/rad/s
Rotor inertia moment	J	$19 \cdot 10^{-6} \text{ kg.m}^2$
Armature Resistance	R	1.835 Ω
Armature Inductance	L	0.287 mH

2.4. PID Controller

PID controller leverages the feedback characteristics of a system to evaluate the accuracy of an instrumentation system. The PID controller is also used to enhance the dynamic response and reduce steady-state errors. The proportional part of PID corrects the change in magnitude depending on the error size, thereby ensuring a fast decrease in the error and providing an initial reaction of the system. Therefore, the integral component of the controller minimizes steady-state errors, whereas the derivative component enhances the transient response (Bistak et al., 2023;

(Bharat et al., 2019; Shah and Agashe, 2016). It has three components: proportional, integral, and derivative. These components can be used individually or simultaneously in any combination depending on the type of plant process or the required response (Ibrahim et al., 2019; Prommee and Angkeaw, 2018; Shah and Agashe, 2016). The transfer function of the PID controller is mathematically represented by Eqs. (34) and (35).

$$k_p + \frac{k_i}{s} + k_d s = \frac{k_d s^2 + k_p s + k_i}{s} \quad (34)$$

$$k_p e + k_i \int e dt + k_d \frac{de}{dt} \quad (35)$$

Several equations are used as error comparison functions to minimize the error value in the PID tuning process. These include integral absolute error (IAE), integral square error (ISE), integral time-weighted square error (ITSE), and integral time-weighted absolute error (ITAE). ITAE is utilized in this system because it provides better performance in delivering smoother and faster responses while also suppressing errors within the system response time. In this case, ITAE is the objective function of optimization performed to obtain the values of k_p , k_i , and k_d in the PID tuning process. The ITAE equation is defined as follows:

$$ITAE = \int_{t=0}^{T_s} t \cdot |e(t)| dt \quad (36)$$

$e(t)$ is the error value at t time, $V(t)$ is the output of the BLDC voltage, $r(t)$ is the set point of the photovoltaic, T_s is the simulation time. Figure 6 shows the whole system block diagram controlled by PID, and Figure 7 depicts the Simulink simulation for optimization.

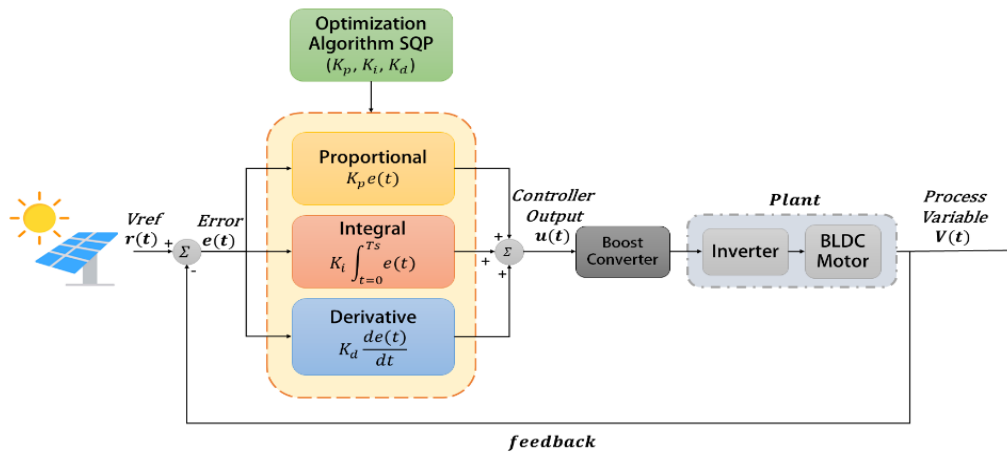


Figure 6 Schematic of the system block diagram

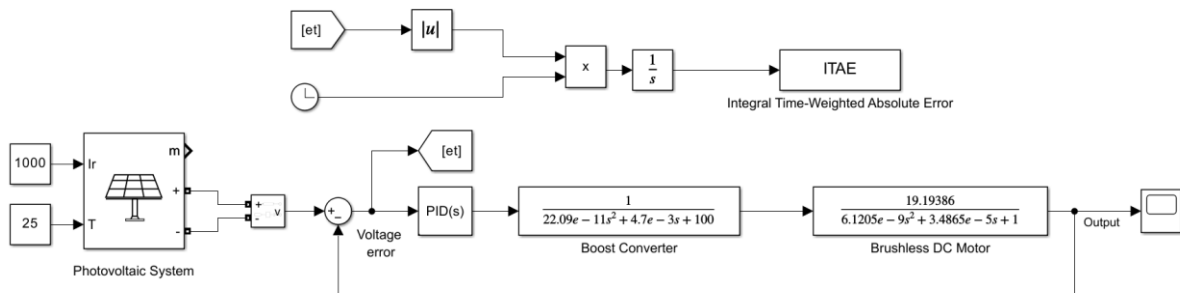


Figure 7 Block diagram for the SQP-PID optimization in Simulink

3. Results and Discussion

This study aims to compare the optimization of the use of several PID models, both conventional and those that have been developed. Based on the findings of several previous studies, several

models were implemented in this study, namely, conventional PID, Geometric Mean Optimizer (GMO), Firefly algorithm (FA), and SQP-PID. The proposed SQP-PID model is a PID controller optimization technique for using a BLDC motor booster converter by considering PV as renewable energy. To support the simulation process, the 200 W solar PV is modeled from electrical parameters in Table 1. This is the initial stage of the simulation process, in which the obtained data can be used as input material for the simulation process in various optimization models. The I-V and P-V characteristic graphs were used in this study. This model provides information related to the system's operational conditions. These characteristics are important indicators for recognizing the PV system's efficiency in producing electricity from sunlight.

The optimization of the PID controller on the DC-DC Boost Converter aims to improve the overall system performance and efficiency. The system can achieve better response characteristics, including faster transient response, reduced settling time, and minimized overshoot or oscillation, by tuning the PID controller parameters, ensuring efficient output voltage regulation under a wide range of load and input conditions. In this system, stability refers to the ability of the generated voltage to reach and maintain an equilibrium state following a disturbance. The disturbance could refer to the uncertainty of photovoltaic. Regardless, instability is characterized by the presence of irregular oscillations and divergence. Conversely, a steady state is achieved when the voltage has stabilized at a constant value, exhibiting no further fluctuations. Optimization helps mitigate stability issues, improving the reliability of operation, especially in renewable energy applications where input source fluctuations are common. Optimized PID controller tuning contributes to increased energy efficiency by minimizing losses and maximizing power conversion efficiency, which is critical for sustainable operation.

This optimization also allows the controller to adapt to changing conditions, maintaining optimal performance across operating conditions, thereby increasing system reliability and robustness while reducing control effort and increasing component longevity. In the optimization process, the simulation block diagram relies on the Simulink feature, as shown in Figure 7. This process aims to obtain the proportional, integral, and derivative values. Figure 8 shows the comparison results among SQP-PID, GMO-PID, and conventional PID simulation. The graph of the simulation results using SQP-PID shows that the rise time obtained by this method is 344 s, whereas the conventional method has a higher value of 649 s. This shows that the SQP-PID model has a faster initial response than the conventional model. The overshoot performance of the SQP-PID model is also better, namely, 0% compared to the conventional model of 11.1%. Additionally, the reduction in completion time between the two is quite significant. The SQP-PID model can be completed in 480 s, whereas the conventional model takes 721 s. The results show that the stability of the SQP-PID model is also better than the conventional model without any excessive deviation.

In addition to the SQP-PID model, other models are also proposed in this study. This aims to obtain the best optimization model among the models used in this study. The next model is the GMO-PID. The simulation results show that the GMO-PID model is almost the same as the SQP-PID model compared with the conventional model. The GMO-PID model has better stability than the conventional model. The GMO-PID overshoot performance has a value of 0%, with a completion time of 529 s. Meanwhile, the GMO-PID rise time value is 379 s. For comparison, the FA-PID model is analyzed in this study. Figure 8 also shows a comparison between the FA-PID model and conventional PID. In this case, the simulation results show that FA-PID has a slower initial response than the conventional model. The FA-PID settling time value in this study is 1108 s. However, the overshoot performance of the FA-PID model decreases significantly to zero with better stability than that of the conventional PID model. In previous research conducted by [Anshory et al. \(2024\)](#), a similar trend was also shown in FA-PID compared with conventional PID. Based on the test results, the SQP-PID model has a better overall value than the GMO-PID, FA-PID, and conventional PID models. However, all optimization models are still better than conventional models in terms of stability when compared with conventional models.

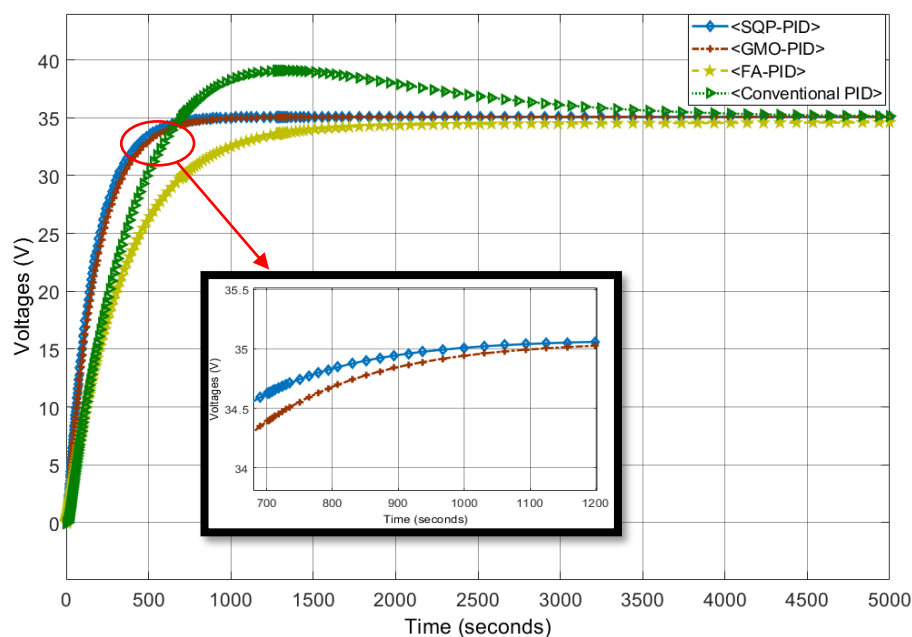


Figure 8 Comparison of PID tuning optimization results

The SQP-PID and GMO-PID models almost give the same value, but not significantly. The difference in values in the model can be seen in the settling time and rise time obtained. SQP – PID has a settling time value of 480 s with a rise time of 344 s, while GMO – PID has a settling time value of 529 s with a rise time of 379 s. Compared with the GMO-PID model, SQP-PID can achieve stability more quickly with a better initial response.

Table 4 presents the performance parameter comparisons resulting from various PID tuning methods, including conventional PID, derivative-based optimization, and metaheuristic-based optimization. The proposed method exhibits a better ITAE value than both the metaheuristic and conventional PID methods. The ITAE achieved is 7.18% and 9.64% smaller than that of FA and GMO, respectively. In addition to the smaller error performance, the time required by the proposed method significantly decreases, being up to 92.45% faster than GMO and 93.91% faster than FA. The simulation time comparison for conventional PID cannot be defined because it utilizes a trial-and-error approach, which is typically more time-consuming than optimization methods, with substantially larger errors.

Table 4 Comparison of various tuning methods

Performance Parameters	Conventional PID	Proposed SQP-PID method	FA-PID (Anshory et al., 2024)	GMO-PID
ITAE	14,892,679.42	1,018,555.64	1,097,300	1,127,200.65
ISE	207,641.55	104,823.75	227,060	114,767.93
ITSE	55,107,347.94	8,409,668.50	4,522,800	10,136,380.24
IAE	15,841.89	5,816.98	14,922	6,364.59
Simulation time (s)	-	55.71	914.49	737.75
Kp	101.44	210	97.76	191.38
Ki	0.08	0.03	0.01	0.02
Kd	-292.72	0.19	-0.13	-4.86
Rise time (s)	649.81	344.66	756.68	379.30
Peak Amplitude	39.08	35.08	34.25	35.07
Settling time (s)	721.73	480.33	1,108	529.18
Overshoot (%)	11.1	0	0	0

4. Conclusions

Based on the results of tests that have been conducted on boost converter planning in all models as a BLDC motor driver using a PID controller, the SQP - PID model as a whole obtained the most superior value compared to other optimization models and conventional PID. This shows that the performance of BLDC motors with a conventional PID controller can be improved by optimizing the PID controller. All optimization methods, especially the proposed SQP-PID model, can reduce the achievement time compared with conventional PID. In this case, the system reaction can increase in achieving work stability as measured by the increase in system speed. The SQP - PID method shows improved performance by reducing completion time by 33.42% compared to conventional PID. Finally, the SQP-PID method decreased significantly from 11.1% to 0% in overshoot performance. Not only did the SQP-PID optimization method decrease, but all optimization methods also decreased to 0%. This indicates that the system is more reliable after optimization methods have been performed to achieve ideal conditions.

Acknowledgements

The Author thanks Universitas Sebelas Maret for the research funding under the scheme "Penelitian Unggulan Terapan (PUT) 2024" under contract number 194.2/UN27.22/PT.01.03/2024.

Author Contributions

Conceptualization, Eki Rovianto; **methodology** Kahirunnisa and Luki Septya Mahendra; **numerical simulation**, Eki Rovianto and Catur Harsito; **validation**, Eki Rovianto and Luki Septya Mahendra; **analysis**, Eki Rovianto; **resources**, Ari Prasetyo; **original draft preparation**, Bhre Wangsa Lenggana and Eki Rovianto; **review and editing**, Eki Rovianto and Catur Harsito; **supervision**, Bhre Wangsa Lenggana and Ari Prasetyo; **project administration**, Eki Rovianto.

Conflict of Interest

The authors have no conflicts of interest to declare.

References

- Aguila-Leon, J, Vargas-Salgado, C, Hurtado-Perez, E, Garcia, EXM & Chiñas-Palacios, C 2021, 'Particle swarm optimization, genetic algorithm and grey wolf optimizer algorithms performance comparative for a DC-DC boost converter PID controller', *Advances in Science, Technology and Engineering Systems Journal*, vol. 6, no. 1, pp. 619-625
- Aiman Setiawan, EAS 2017, 'Optimization of a photovoltaic power plant in Indonesia with proper tilt angle and photovoltaic type using a system advisor model', *International Journal of Technology*, vol. 8, no. 3, pp. 291-319, <https://doi.org/10.14716/ijtech.v8i3.8076>
- Ajiwiguna, TA & Kirom, MR 2024, 'Uninterrupted electricity supply using off-grid solar PV systems for remote areas', *International Journal of Technology*, vol. 15, no. 5, pp. 1561-1572, <https://doi.org/10.14716/ijtech.v15i5.6089>
- Alshareef, A, Shah, R, Mithulananthan, N & Alzahrani, S 2021, 'A new global index for short term voltage stability assessment', *IEEE Access*, vol. 9, pp. 36114-36124, <https://doi.org/10.1109/ACCESS.2021.3061712>
- Anshory, I, Jamaaluddin, J, Wisaksono, A, Sulistiyowati, I, Hindarto, Rintyarna, BS, Fudholi, A, Rahman, YA & Sopian, K 2024, 'Optimization DC-DC boost converter of BLDC motor drive by solar panel using PID and firefly algorithm', *Results in Engineering*, vol. 21, article 101727, <https://doi.org/10.1016/j.rineng.2023.101727>
- Aseem, K & Selva Kumar, S 2020, 'Closed loop control of DC-DC converters using PID and FOPID controllers', *International Journal of Power Electronics and Drive Systems*, vol. 11, no. 3, pp. 1323-1332, <https://doi.org/10.11591/ijpeds.v11.i3.pp1323-1332>
- Ben Safia, Z, Kharrat, M, Allouche, M & Mohamed, C 2021, 'TS fuzzy fault-tolerant tracking control of a PV pumping system based on an induction motor', *IETE Journal of Research*, vol. 7, pp. 4826-4835, <https://doi.org/10.1080/03772063.2021.1958387>

Bharat, S, Ganguly, A, Chatterjee, R, Basak, B, Sheet, DK & Ganguly, A 2019, 'A review on tuning methods for PID controller', *Asian Journal for Convergence in Technology*, vol. 5, no. 1, pp. 1-4, <http://www.asianssr.org/index.php/ajct/article/view/731>

Bistak, P, Huba, M, Vrancic, D & Chamraz, S 2023, 'IPDT model-based Ziegler–Nichols tuning generalized to controllers with higher-order derivatives', *Sensors*, vol. 23, no. 8, article 3787, <https://doi.org/10.3390/s23083787>

Bueso, MC, Paredes-Parra, JM, Mateo-Aroca, A & Molina-García, A 2022, 'Sensitive parameter analysis for solar irradiance short-term forecasting: Application to LoRa-based monitoring technology', *Sensors*, vol. 22, no. 4, article 1499, <https://doi.org/10.3390/s22041499>

De, S, Swathika, OVG, Tewari, N, Venkatesan, AK, Subramaniam, U, Bhaskar, MS, Padmanaban, S, Leonowicz, Z & Mitolo, M 2020, 'Implementation of designed PV integrated controlled converter system', *IEEE Access*, vol. 8, pp. 100905-100915, <https://doi.org/10.1109/ACCESS.2020.2997405>

Delfianti, R, Rovianto, E, Budi, ALS, Priyadi, A, Abadi, I & Soeprijanto, A 2022, 'Evaluation of the energy transaction cost for microgrid-based wheeling system using power flow tracing: A case study', *International Review of Electrical Engineering*, vol. 17, no. 2, pp. 154-163, <https://doi.org/10.15866/iree.v17i2.21792>

Devaraj, SV, Gunasekaran, M, Sundaram, E, Venugopal, M, Chenniappan, S, Almakhlles, DJ, Subramaniam, U & Bhaskar, MS 2021, 'Robust queen bee assisted genetic algorithm (QBGA) optimized fractional order PID (FOPID) controller for not necessarily minimum phase power converters', *IEEE Access*, vol. 9, pp. 93331-93337, <https://doi.org/10.1109/ACCESS.2021.3092215>

Eleftheratos, K, Raptis, I-P, Kouklaki, D, Kazadzis, S, Founda, D, Psiloglou, B, Kosmopoulos, P, Fountoulakis, I, Benetatos, C, Gierens, K, Kazantzidis, A, Richter, A & Zerefos, C 2024, 'Atmospheric parameters affecting spectral solar irradiance and solar energy (ASPIRE)', *AIP Conference Proceedings*, vol. 2988, no. 1, article 110002, <https://doi.org/10.1063/5.0183678>

Gao, Y 2023, 'PID-based search algorithm: A novel metaheuristic algorithm based on PID algorithm', *Expert Systems with Applications*, vol. 232, article 120886, <https://doi.org/10.1016/j.eswa.2023.120886>

Ghamari, SM, Narm, HG & Mollaei, H 2022, 'Fractional-order fuzzy PID controller design on buck converter with antlion optimization algorithm', *IET Control Theory & Applications*, vol. 16, no. 3, pp. 340-352, <https://doi.org/10.1049/cth2.12230>

Grigoraş, G, Neagu, B-C, Ivanov, O, Livadariu, B & Scarlatache, F 2022, 'A new SQP methodology for coordinated transformer tap control optimization in electric networks integrating wind farms', *Applied Sciences*, vol. 12, no. 3, article 1129, <https://doi.org/10.3390/app12031129>

Hasanah, RN, Yuniar, F, Setyawati, O, Suyono, H, Sawitri, DR & Taufik, T 2024, 'A modified perturb-and-observe control for improved maximum power point tracking performance on grid-connected photovoltaic system', *International Journal of Technology*, vol. 15, no. 1, pp. 291-319, <https://doi.org/10.14716/ijtech.v15i1.5316>

Hekimoğlu, B & Ekinci, S 2020, 'Optimally designed PID controller for a DC-DC buck converter via a hybrid whale optimization algorithm with simulated annealing', *Electrica*, vol. 20, no. 1, pp. 19-27, <https://doi.org/10.5152/electrica.2020.19034>

Ibrahim, MA, Mahmood, AK & Sultan, NS 2019, 'Optimal PID controller of a brushless DC motor using genetic algorithm', *International Journal of Power Electronics and Drive Systems (IJPEDS)*, vol. 10, no. 2, pp. 822-830, <https://doi.org/10.11591/ijpeds.v10.i2.pp822-830>

Izci, D, Hekimoğlu, B & Ekinci, S 2022, 'A new artificial ecosystem-based optimization integrated with Nelder-Mead method for PID controller design of buck converter', *Alexandria Engineering Journal*, vol. 61, no. 3, pp. 2030-2044, <https://doi.org/10.1016/j.aej.2021.07.037>

Jamahori, HF, Abdullah, MP, Ali, A & AlKassem, A 2024, 'Optimal design and performance analysis of multiple photovoltaic with grid-connected commercial load', *International Journal of Technology*, vol. 15, no. 4, pp. 291-319, <https://doi.org/10.14716/ijtech.v15i4.6019>

Janprom, K, Permpoonsinsup, W & Wangnipparnto, S 2020, 'Intelligent tuning of PID using metaheuristic optimization for temperature and relative humidity control of comfortable rooms', *Journal of Control Science and Engineering*, vol. 2020, no. 1, article 2596549, <https://doi.org/10.1155/2020/2596549>

Jia, Y, Alva, G & Fang, G 2019, 'Development and applications of photovoltaic–thermal systems: A review', *Renewable and Sustainable Energy Reviews*, vol. 102, pp. 249-265, <https://doi.org/10.1016/j.rser.2018.12.030>

Joseph, SB, Dada, EG, Abidemi, A, Oyewola, DO & Khammas, BM 2022, 'Metaheuristic algorithms for PID controller parameters tuning: Review, approaches and open problems', *Helijon*, vol. 8, no. 5, article e09399, <https://doi.org/10.1016/j.helijon.2022.e09399>

- Khleaf, HK, Nahar, AK & Jabbar, AS 2019, 'Intelligent control of DC-DC converter based on PID-neural network', *International Journal of Power Electronics and Drive Systems (IJPEDS)*, vol. 10, no. 4, pp. 2254-2262
- Khodabakhshian, A, Pour, ME & Hooshmand, R 2012, 'Design of a robust load frequency control using sequential quadratic programming technique', *International Journal of Electrical Power & Energy Systems*, vol. 40, no. 1, pp. 1-8, <https://doi.org/10.1016/j.ijepes.2011.10.018>
- Kumar, PP & Vinaykumar, M 2023, 'A review on the estimate solar PV cell variables for efficient photovoltaic systems', *International Journal of Smart Grid*, vol. 7, no. 3
- Liu, Ye, Qian, Y, Feng, S, Berg, LK, Juliano, TW, Jiménez, PA, Gritmit, E & Liu, Y 2022, 'Calibration of cloud and aerosol related parameters for solar irradiance forecasts in WRF-solar', *Solar Energy*, vol. 241, pp. 1-12, <https://doi.org/10.1016/j.solener.2022.05.064>
- Luo, X-L, Lv, J-H & Sun, G 2022, 'Continuation methods with the trusty time-stepping scheme for linearly constrained optimization with noisy data', *Optimization and Engineering*, vol. 23, no. 1, pp. 329-360, <https://doi.org/10.1007/s11081-020-09590-z>
- Malla, SG, Malla, P, Malla, JMR, Singla, R, Choudekar, P, Koilada, R & Sahu, MK 2022, 'Whale optimization algorithm for PV based water pumping system driven by BLDC motor using sliding mode controller', *IEEE Journal of Emerging and Selected Topics in Power Electronics*, vol. 10, no. 4, pp. 4832-4844, <https://doi.org/10.1109/JESTPE.2022.3150008>
- Mao, T, Zhang, X & Zhou, B 2019, 'Intelligent energy management algorithms for EV-charging scheduling with consideration of multiple EV charging modes', *Energies*, vol. 12, no. 2, article 265, <https://doi.org/10.3390/en12020265>
- MathWorks 2004, *MATLAB R2024b*, Natick, MA, The MathWorks, Inc.
- Miqoi, S, El Ougli, A & Tidhaf, B 2019, 'Adaptive fuzzy sliding mode based MPPT controller for a photovoltaic water pumping system', *International Journal of Power Electronics and Drive Systems (IJPEDS)*, vol. 10, no. 1, pp. 414-422, <https://doi.org/10.11591/ijped.v10.i1.pp414-422>
- Mitra, L & Rout, UK 2022, 'Optimal control of a high gain DC-DC converter', *International Journal of Power Electronics and Drive Systems (IJPEDS)*, vol. 13, no. 1, pp. 256-266, <https://doi.org/10.11591/ijped.v13.i1.pp256-266>
- Mohammed, H & Farah, N 2019, 'Photovoltaic (PV) system applied to induction motor drives', *International Journal of Advanced Science and Technology*, vol. 28, no. 1, pp. 363-373
- Mohasseb, S, Moradi, M, Sokhansefat, T, Kowsari, F, Kasaeian, A & Mahian, O 2017, 'A novel approach to solve inverse heat conduction problems: Coupling scaled boundary finite element method to a hybrid optimization algorithm', *Engineering Analysis with Boundary Elements*, vol. 84, pp. 206-212, <https://doi.org/10.1016/j.enganabound.2017.08.018>
- Munisekhar, S, Marutheeswar, GV, Sujatha, P & Vadivelu, KR 2020, 'A novel approach for the fastest MPPT tracking algorithm for a PV array fed BLDC motor driven air conditioning system', *Indonesian Journal of Electrical Engineering and Computer Science*, vol. 18, no. 2, pp. 622-628, <http://doi.org/10.11591/ijeecs.v18.i2.pp622-628>
- Nasruddin & Sinambela, H 2015, 'Design and experimental study of air conditioning system using brushless direct current (BLDC) compressor in national electric car', *International Journal of Technology*, vol. 6, no. 6, pp. 954-960, <https://doi.org/10.14716/ijtech.v6i6.1896>
- Obaid, W, Hamid, A-K & Ghenai, C 2021, 'Hybrid solar/wind/diesel water pumping system: A case study in Dubai United Arab Emirates', *International Journal of Electrical and Computer Engineering*, vol. 11, no. 3, pp. 2062-2067, <https://doi.org/10.11591/ijece.v11i3.pp2062-2067>
- Osman, N, Khalid, HM, Sweidan, TO, Abuashour, MI & Muyeen, SM 2022, 'A PV powered DC shunt motor: Study of dynamic analysis using maximum power point-based fuzzy logic controller', *Energy Conversion and Management: X*, vol. 15, article 100253, <https://doi.org/10.1016/j.ecmx.2022.100253>
- Osorio, EdIR, Becerra, GN, Palafox-Roca, AO & Ledesma-Alonso, R 2019, 'An empiric-stochastic approach, based on normalization parameters, to simulate solar irradiance', *Journal of Solar Energy Engineering*, vol. 141, no. 6, article 061011, <https://doi.org/10.1115/1.4043863>
- Prommee, P & Angkeaw, K 2018, 'High performance electronically tunable log-domain current-mode PID controller', *Microelectronics Journal*, vol. 72, pp. 126-137, <https://doi.org/10.1016/j.mejo.2017.09.008>
- Saaid, FI, Tseng, T-Y & Winie, T 2018, 'PVdF-HFP quasi-solid-state electrolyte for application in dye-sensitized solar cells', *International Journal of Technology*, vol. 9, no. 6, pp. 1187-1195, <https://doi.org/10.14716/ijtech.v9i6.2344>
- Shah, P & Agashe, S 2016, 'Review of fractional PID controller', *Mechatronics*, vol. 38, pp. 29-41, <https://doi.org/10.1016/j.mechatronics.2016.06.005>

Sugiantoro, N, Wibowo, RS, Lystianingrum, V, Rovianto, E & Triwijaya, S 2021, 'Optimal power flow with dynamic line rating using quadratically constrained quadratic program method', *In: Proceedings of the 1st International Conference on Electronic and Electrical Engineering and Intelligent System (ICE3IS)*, pp. 54-59

Wibowo, RS, Rovianto, E, Lystianingrum, V, Aryani, NK & Penangsang, O 2023, 'Dynamic optimal power flow for microgrids considering efficiency and lifetime of battery using MINLP', *International Review of Electrical Engineering*, vol. 18, no. 1, pp. 15-24, <https://doi.org/10.15866/iree.v18i1.22466>